Progress In Electromagnetics Research Letters, Vol. 88, 15–20, 2020

Wideband Low-Profile Dual-Polarized Antenna with AMC Reflector

Alexander P. Volkov[1, *], Vitalii V. Kakshin[1], Igor Yu. Ryzhov[1], Kirill V. Kozlov[1], and Alexander Yu. Grinev[2]

Abstract—A wideband low-profile dual-polarized antenna based on the use of an artificial magnetic conductor (AMC) reflector is proposed. The AMC reflector consists of 9×9 square patches. In order to obtain wide impedance and gain bandwidths, the antenna consists of four printed dipoles: two dipoles are used as a radiator of horizontal polarization, and two dipoles are used as a radiator of vertical polarization. A simple excitation scheme without balun is used for dipoles feeding. A low profile of $0.068\lambda_L$ is realized (λ_L is the wavelength at the lowest operating frequency). Simulation and measurement results show that the proposed antenna has a 40% impedance bandwidth, a 40% 3-dB gain bandwidth, and a port isolation of less than -30 dB.

1. INTRODUCTION

The rapid development of radio electronic devices, especially synthetic aperture radars (SARs) [1] and wireless communication systems [2, 3], requires dual-polarized antennas with a low-profile, wide bandwidth, and high port isolation. For instance, in an aviation SAR antenna profile lowering preserves aircraft aerodynamics. In space SAR, it is important to have a low profile antenna for compact arrangement inside a radome of the rocket launching into Earth's orbit.

Periodic structures play an important role for an antenna characteristics improvement [4–6]. Artificial magnetic conductors (AMCs) are widely used for profile reduction of dipole antennas placed parallel to a ground plane [7]. However, a radiation pattern of the antenna based on an AMC degrades in a wide frequency band because of surface wave excitation in a finite AMC [8]. Different methods can be use to decrease the aforementioned effect [9–19]. A reduction of AMC unit cell numbers prevents surface wave excitation [9–11]. The single polarized antenna based on the AMC reflector consists of 8×6 units has the profile height of $0.033\lambda_L$ and bandwidth of 36.78% was presented in [10]. An additional gap between the AMC and the antenna can decrease coupling between them and enhance the antenna radiation pattern [12–15]. The dual-polarized antenna with the AMC reflector height of $0.024\lambda_L$, the distance between the AMC and the radiator of $0.04\lambda_L$ has bandwidth of 22.3% was designed in [14]. Hybrid reflectors, consisting of an AMC and metallic strips or walls, have been proposed to mitigate this problem [16, 17]. For instance, in [17] the dual-polarized antenna has the profile height of $0.098\lambda_L$ and bandwidth of 54.8% was presented. Excitation schemes using two dipoles to improve the antenna radiation pattern have been proposed in [18, 19]. In [19] the single polarized antenna using a pair of dipoles has the profile height of $0.087\lambda_L$, and the bandwidth of 45% was proposed.

In this paper, a wideband, dual-polarized antenna with a low profile is presented for a synthetic aperture radar of an unmanned aerial vehicle. The AMC reflection phase and dispersion diagram are analysed. The prototype of the proposed antenna is constructed and measured. The key parameters of the antenna is compared with the antennas, presented in state-of-the-art literature.

Received 7 October 2019, Accepted 19 November 2019, Scheduled 30 November 2019

* Corresponding author: Alexander P. Volkov (alexander.p.volkov@gmail.com).

[1] JSC Corporation VEGA, Moscow, Russia. [2] Moscow Aviation Institute (National Research University), Moscow, Russia.

2. ANTENNA DESIGN

2.1. Antenna Geometry

The 3D view of the antenna is depicted in Figure 1. The antenna consists of two dielectric layers. The layers are separated by four plastics bolts.

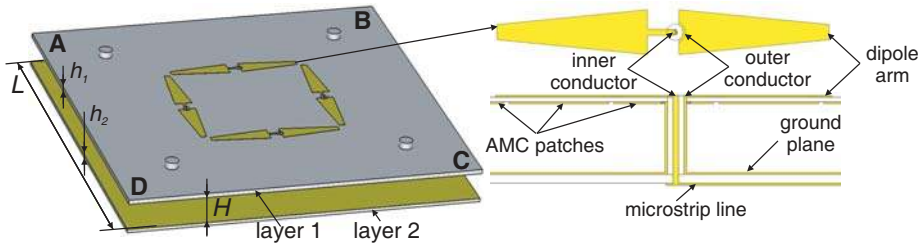

Figure 1. 3D view of the presented antenna.

The radiators (Figure 2(a)) and AMC (Figure 2(b)) topologies are etched on different sides of the layer 1 (RO4350B, the thickness of $h_1 = 0.762$ mm). Four dipoles are used as radiating elements have the following parameters: $dl = 57.5$ mm, $dw_1 = 7.75$ mm, $dw_2 = 2.55$ mm, $dg = 5.5$ mm, $T = 62.5$ mm, $L = 161.32$ mm. Each dipole is fed by a coaxial cable (SF-086). A balun was not used in the design in order to simplify the antenna construction. However it could enhance a polarization purity of the antenna. Coaxial cables are electrically isolated with the AMC patches. One of the dipole arms is connected to an outer coaxial conductor and another dipole arm is connected to an inner coaxial conductor. The AMC consists of 9×9 square patch elements with key parameters of: $w = 17.1$ mm, $D = 17.98$ mm, $r = 2.2$ mm. The topology of the antenna feeding network (Figure 2(c)) is etched on the bottom side of the layer 2 (RO4350B, the thickness of $h_2 = 1.524$ mm). Another side of the layer 2 is used as the antenna ground plane. 3-dB power dividers are used for dipole feeding. The key parameters of the antenna feeding network are: $fw = 3.35$ mm, $fw_1 = 1.84$ mm, $dl_1 = 22.2$ mm. The distance between two substrates is $H = 12.0$ mm.

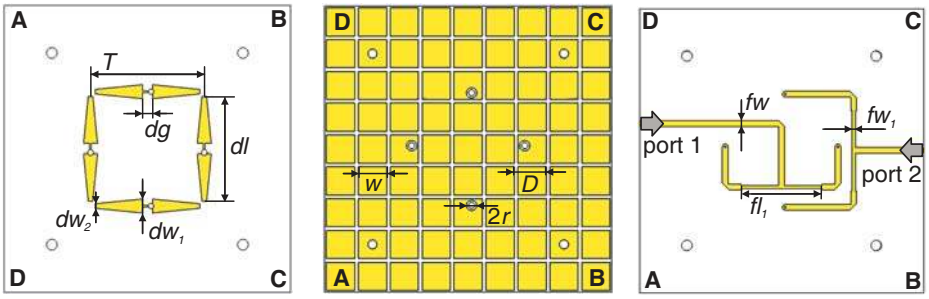

(a) (b) (c)

Figure 2. Geometry of the antenna layers. (a) Top view of the layer, 1, (b) bottom view of the layer 1, (c) bottom view of the layer 2.

One of the important parameters of the presented antenna is the distance T between pairs of dipoles. Figure 3 shows the simulated directivity versus frequency in the broadside direction for different T. It can be seen that the broadside directivity tends to have a dip while T is decreased.

2.2. AMC Design

An AMC reflector plays an important role for profile lowering and bandwidth widering of an antenna. The geometry of the selected AMC unit is shown in Figure 4(a). The phase reflection was simulated

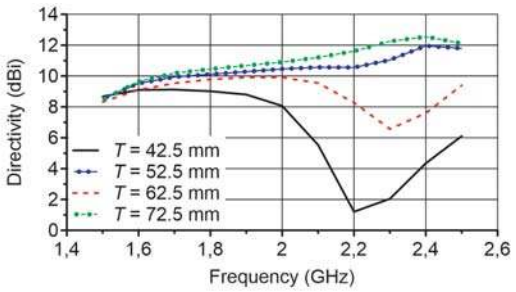

Figure 3. Simulated antenna directivity in the broadside direction.

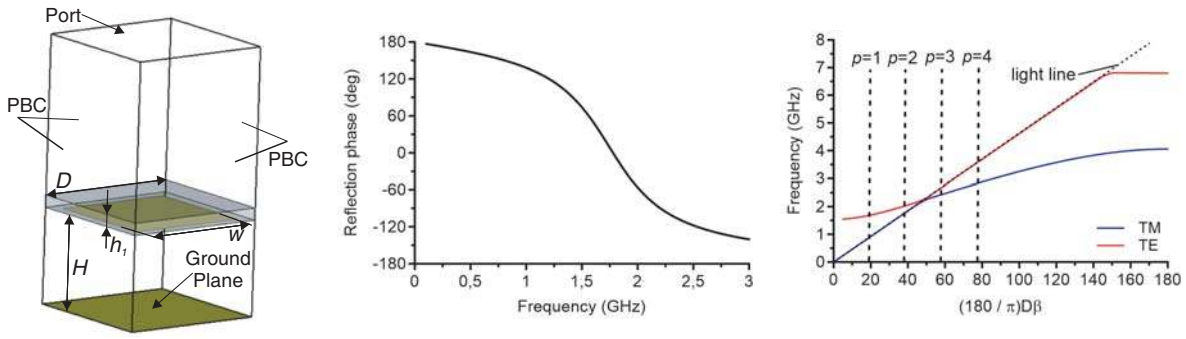

(a) (b) (c)

Figure 4. AMC reflector design. (a) AMC unit, (b) reflection phase, (c) dispersion diagram.

using periodic boundary conditions. Figure 4(b) shows that the resonance frequency of the AMC is at 1.7 GHz. In order to obtain a wideband impedance bandwidth, surface wave can be exited into finite AMC reflector [8, 18, 19]. The AMC reflector with 9×9 square patch elements was chosen to provide it. Figure 4(c) shows the dispersion diagram of the AMC. The TM and TE modes were simulated. The TE mode and the light line are very closely to each other because of the AMC air spacer. It crosses the light line at 2.66 GHz. Surface wave resonances occur when the TE mode or TM curves intersect with vertical lines representing the quantity $p\pi/ND$ (N is a number of AMC unit cells, $p = 1, 2, \ldots$) [8]. It can be seen that the first resonances occur when $p = 3$. The TM mode resonance is at 2.41 GHz, and the TE mode resonance is at 2.68 GHz.

3. RESULTS

The antenna is constructed to approve the simulation results. The prototype is shown in Figure 5. Finite elements method was used to simulate the performance of the antenna. Nelder Mead Simplex Algorithm was used to optimize the antenna characteristics.

The antenna S-parameters are measured by the Agilent PNA-X network analyzer. The simulated and measured $|S_{11}|$ and $|S_{22}|$ are depicted in Figure 6(a). The impedance bandwidth is about 40% (1.6–2.4 GHz) for $|S_{ii}| \leq -10$ dB. Figure 6 (a) shown that the antenna has two resonances at 1.65 GHz and at 2.4 GHz. The first resonance associates with the dipoles resonance and the second resonance associates with the AMC reflector resonance. The simulated and measured $|S_{21}|$ is depicted in Figure 6(b). The isolation is lower than -30 dB from 1.6 to 2.4 GHz. The simulation results of S-parameters are well matched with the experimental results.

The realized gains and radiation patterns of the antenna are measured by a planar near field method into an anechoic chamber. The simulated and measured realized gains for ports 1 and 2 are depicted in Figure 7(a). The simulated and measured realized gains are $9 \ldots 11$ dBi and $9 \ldots 12$ dBi over the higher band respectively. The deterioration of measured gains is mainly caused by the loss of coaxial cable and the SMA connectors. Figure 7(b) shows the antenna efficiency. The simulated efficiencies are $89 \ldots 97\%$

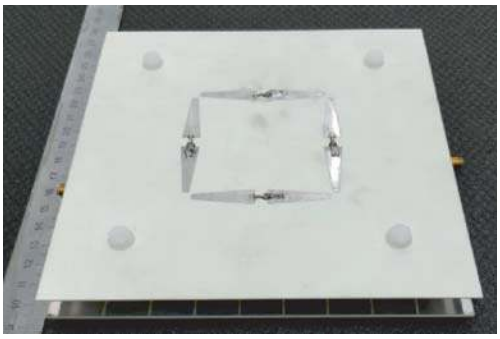

Figure 5. Manufactured prototype of the antenna.

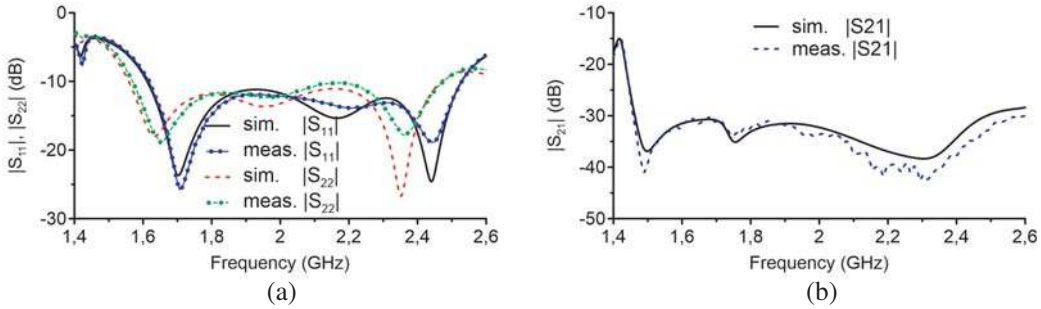

Figure 6. Simulated and measured (a) $|S_{11}|$ and $|S_{22}|$, (b) $|S_{21}|$ of the presented antenna.

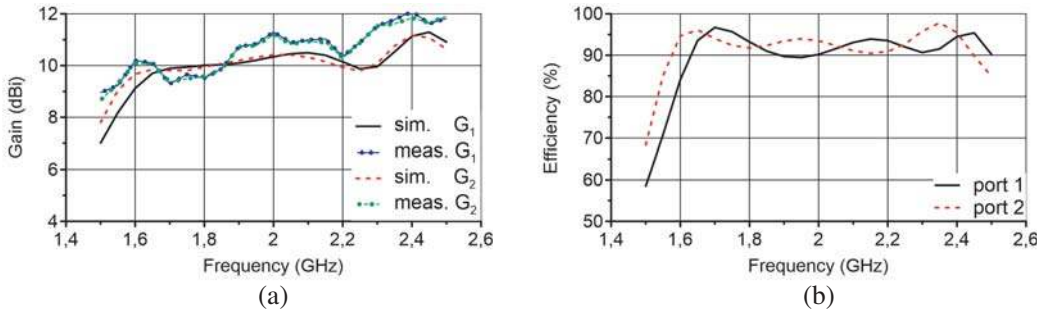

Figure 7. (a) Simulated and measured realized gain, (b) antenna efficiency.

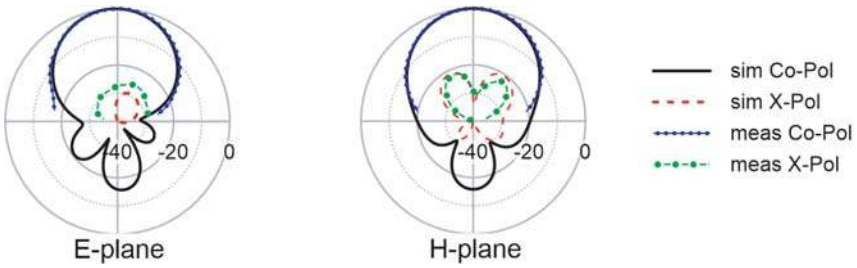

Figure 8. Simulated and measured normalized radiation patterns for port 1 at 2 GHz.

from 1.6 to 2.4 GHz for ports 1 and 2. The simulated and measured normalized radiation patterns for ports 1 and 2 are depicted in Figure 8 and Figure 9 at 2 GHz respectively. The simulated and measured the HPBWs are 49 . . . 65° and 43 . . . 56° in E-plane and H-plane of the antenna for ports 1 and 2. The simulated F/B ratio is better of 11 dB for both antenna ports.

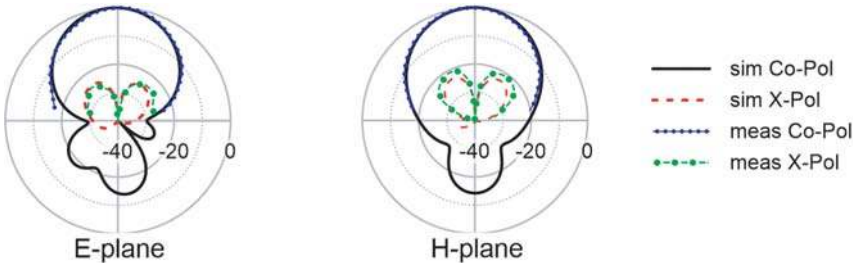

Figure 9. Simulated and measured normalized radiation patterns for port 2 at 2 GHz.

Table 1 compares the key features of the proposed antenna and the antennas presented in state-of-the-art literature [9–19]. In comparison with [9, 10, 11, 16, 18, 19], the presented antenna operates at two orthogonal polarizations. It has lesser profile height and comparable bandwidth than the antennas presented in [12–15]. In comparison with [19], the proposed antenna has simpler feeding scheme without a balun and an impedance matching network.

Table 1. Comparison of the proposed and previous antennas.

Design cases	Profile height	Bandwidth	Polarization
[9]	$0.05\lambda_L$	36.7%	Linearly polarized
[10]	$0.033\lambda_L$	36.78%	Linearly polarized
[11]	$0.026\lambda_L$	18%	Linearly polarized
[12]	$0.11\lambda_L$	33%	Dual-polarized
[13]	$0.11\lambda_L$	26.5%	Dual-polarized
[14]	$0.12\lambda_L$	54%	Dual-polarized
[15]	$0.064\lambda_L$	22.3%	Dual-polarized
[16]	$0.077\lambda_L$	46%	Linearly polarized
[17]	$0.098\lambda_L$	54.8%	Dual-polarized
[18]	$0.075\lambda_L$	40%	Linearly polarized
[19]	$0.087\lambda_L$	45%	Linearly polarized
[Proposed antenna]	$0.068\lambda_L$	40%	Dual-polarized

4. CONCLUSION

A wideband low-profile dual-polarized antenna with an AMC reflector has been proposed. By using the AMC reflector, the antenna obtains a low profile and wide bandwidth. By using two dipoles as a radiator for horizontal or vertical polarizations, the antenna has a wide 3-dB gain bandwidth and good port isolation. The simulated and measured results indicate that the antenna has a low profile of $0.068\lambda_L$ while an impedance bandwidth of 40% and 3-dB gain bandwidth of 40%. Port isolation, lower than -30 dB, is achieved. Compared with the known dual-polarized antennas using an AMC reflector, the proposed antenna has a lower profile with a comparable impedance bandwidth. The antenna was designed for a synthetic aperture radar of an unmanned aerial vehicle.

REFERENCES

1. Alibakhshi-Kenari, M., B. S. Virdee, and E. Limiti, "Wideband planar array antenna based on SCRLH-TL for airborne synthetic aperture radar application," *Journal of Electromagnetic Waves and Applications*, Vol. 61, No. 2, 524–531, 2018.

2. Alibakhshi-Kenari, M., B. S. Virdee, C. H. See, R. Abd-Alhameed, A. Ali, F. Falcone, and E. Limiti, "Wideband printed monopole antenna for application in wireless communication systems," *IET Microw. Antennas Propag.*, Vol. 61, No. 2, 524–531, 2018.
3. Cui, Y., X. N. Gao, H. Z. Fu, Q. X. Chu, and R. L. Li, "Broadband dual-polarized dual-dipole planar antennas: Analysis, design, and application for base stations," *Antennas Propag. Mag.*, Vol. 59, No. 6, 77–87, 2017.
4. Abegaonkar, M., L. Kurra, and S. K. Koul, *Printed Resonant Periodic Structures and Their Applications*, CRC Press, USA, Florida, Boca Raton, 2016.
5. Alibakhshi-Kenari, M., M. Naser-Moghadasi, R. A. Sadeghzadeh, B. S. Virdee, and E. Limiti, "Periodic array of complementary artificial magnetic conductor metamaterials-based multiband antennas for broadband wireless transceivers," *IET Microw. Antennas Propag.*, Vol. 10, No. 15, 1682–1691, 2016.
6. Alibakhshi-Kenari, M., M. Naser-Moghadasi, B. S. Virdee, A. Andujar, and J. Anguera, "Compact antenna based on a composite right/left handed transmission line," *Microw. Opt. Technol. Lett.*, Vol. 57, No. 8, 1785–1788, 2015.
7. Yang, F. and Y. Rahmat-Samii, *Electromagnetic Band Gap Structures in Antenna Engineering*, Cambridge University Press, New York, USA, 2009.
8. Costa, F., O. Luukkonen, C. R. Simovski, A. Monorchio, S. A. Tretyakov, and P. M. de Maagt, "TE surface wave resonances on high-impedance surface based antenna: Analysis and modeling," *IEEE Trans. Antennas Propag.*, Vol. 59, No. 10, 3588–3596, 2011.
9. Li, X., Y.-C. Jiao, and L. Zhang, "Wideband low-profile CPW-fed slot-loop antenna using an artificial magnetic conductor," *IET Electronics Letters*, Vol. 54, No. 11, 673–674, 2018.
10. Azad, M. Z. and M. Ali, "Novel wideband directional dipole antenna on a mushroom like EBG structure," *IEEE Trans. Antennas and Propag.*, Vol. 56, No. 2, 1242–1250, 2008.
11. Raad, H. R., A. I. Abbosh, H. M. Al-Rizzo, and D. G. Rucker, "Flexible and compact AMC based antenna for telemedicine applications," *IEEE Trans. Antennas and Propag.*, Vol. 61, No. 2, 524–531, 2013.
12. Li, G., H. Zhai, L. Li, C. Liang, R. Yu, and S. Liu, "AMC-loaded wideband base station antenna for indoor access point in MIMO system," *IEEE Trans. Antennas and Propag.*, Vol. 63, No. 2, 525–533, 2015.
13. Ren, J., B. Wang, and Y.-Z. Yin, "Low profile dual-polarized circular patch antenna with an AMC reflector," *Progress In Electromagnetics Research Letters*, Vol. 47, 131–137, 2014.
14. Zhai, H., L. Xi, L. X. Zang, and Z. N. Chen, "A low profile dual-polarized high isolation MIMO antenna arrays for wideband base station applications," *IEEE Trans. Antennas and Propag.*, Vol. 66, No. 1, 191–202, 2018.
15. Zhu, K., M. Su, C. Yu, and Y. Liu, "Compact high-isolation dual-polarized antenna with AMC reflector," *Progress In Electromagnetics Research M*, Vol. 73, 1–8, 2018.
16. Joshi, C., A. C. Lepage, J. Sarrazin, and X. Begaud, "Enhanced broadside gain of an ultra-wide band diamond dipole antenna using a hybrid reflector," *IEEE Trans. Antennas and Propag.*, Vol. 64, No. 7, 3269–3274, 2016.
17. Li, M., Q. L. Li, B. Wang, C. F. Zhou, and S. W. Cheung, "A low-profile dual-polarized dipole antenna using wideband AMC reflector," *IEEE Trans. Antennas and Propag.*, Vol. 66, No. 5, 2610–2615, 2018.
18. Volkov, A. P., K. V. Kozlov, A. P. Kurochkin, and A. Yu. Grinev, "Enhanced directivity of low-profile wideband antenna based on artificial magnetic conductor," *Radiation and Scattering of Electromagnetic Waves (RSEMW)*, 2179–2184, Divnomorskoe, Russia, June 2017.
19. Lin, F. H. and Z. N. Chen, "Truncated impedance-sheet model for low-profile broadband non-resonant-cell metasurface antennas using characteristic mode analysis," *IEEE Trans. Antennas and Propag.*, Vol. 66, No. 10, 5043–5051, 2018.